Impedance of finite length resistive cylinder

S. Krinsky and B. Podobedov
Brookhaven National Laboratory, Upton, New York 11973, USA

R. L. Gluckstern
Department of Physics, University of Maryland, College Park, Maryland 20742, USA
(Received 15 July 2004; published 8 November 2004)

We determine the impedance of a cylindrical metal tube (resistor) of radius a, length g, and conductivity σ attached at each end to perfect conductors of semi-infinite length. Our main interest is in the asymptotic behavior of the impedance at high frequency ($k \gg 1/a$). In the equilibrium regime, $ka^2 \ll g$, the impedance per unit length is accurately described by the well-known result for an infinite length tube with conductivity σ. In the transient regime, $ka^2 \gg g$, where the contribution of transition radiation arising from the discontinuity in conductivity is important, we derive an analytic expression for the impedance and compute the short-range wakefield. The analytic results are shown to agree with numerical evaluation of the impedance.

DOI: 10.1103/PhysRevSTAB.7.114401 PACS numbers: 41.20.Jb, 41.60.–m

I. INTRODUCTION

We consider the longitudinal impedance of a cylindrical metal tube (resistor) of radius a, length g, and conductivity σ attached at each end to perfect conductors of semi-infinite length (Fig. 1). Our main interest is in the high frequency behavior, $k = \omega/c \gg 1/a$. There are two regimes: (i) When the Rayleigh range ka^2 corresponding to the tube radius is short compared to the resistor length g, the field pattern settles into an equilibrium in which the field is continually being eaten at the resistor while it is being replenished on axis by the deceleration of the beam [1]. In this case, the impedance per unit length is well approximated by that of an infinite length tube with conductivity σ [2–5]. (ii) When the Rayleigh range ka^2 is short compared to g, equilibrium is not reached and the impedance per unit length differs from that of an infinite tube. We present an analytic description of the impedance in this transient regime. Our discussion is complementary to the recent work of Ivanyan and Tsakanov [6].

Our approach is based on an integral equation for the longitudinal electric field in the resistor. In the transient regime, the kernel of this equation can be simplified [7], and analytic asymptotic results obtained. In the general case, the integral equation can be solved by expanding the field in a Fourier series in the axial coordinate z, and deriving an infinite set of linear algebraic equations for the Fourier coefficients. Truncating these equations by keeping only a limited number of Fourier components, the equations can be solved numerically.

Let us write the impedance in the form

$$Z(a, g; k) = \frac{Z_s(k) g}{2\pi a} G(a, g; k), \tag{1.1}$$

where the surface impedance Z_s is defined by (mks units, $Z_0 = 1/\varepsilon_0 c$, and $j = \sqrt{-1}$)

$$Z_s(k) = (1 + j) Z_0 \sqrt{\frac{k}{2\sigma Z_0}}, \qquad (k > 0). \tag{1.2}$$

Branch cuts are chosen such that $Z^*(a, g; k) = Z(a, g; -k)$ and $Z_s^*(k) = Z_s(-k)$. In the case $ka^2 \ll g$, the impedance per unit length is well approximated by that of an infinite cylinder with conductivity σ [2–5], so

$$G \cong G_\infty(ks_0) = \frac{1}{1 + \frac{1}{4}(j - 1)(ks_0)^{3/2}}, \tag{1.3}$$

where s_0 is the characteristic length discussed in [3–5],

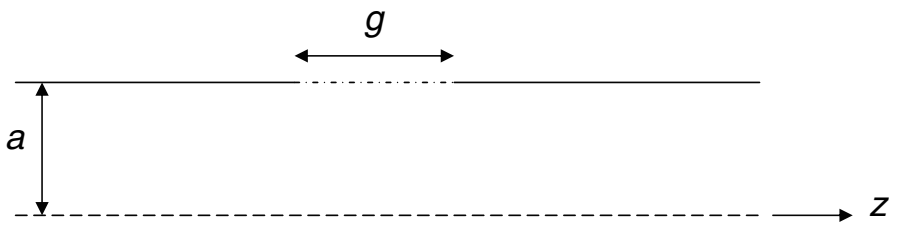

FIG. 1. Cylindrical tube of radius a, having finite conductivity σ in a section of length g, and infinite conductivity outside this interval.

 1098-4402/04/7(11)/114401(9)$22.50

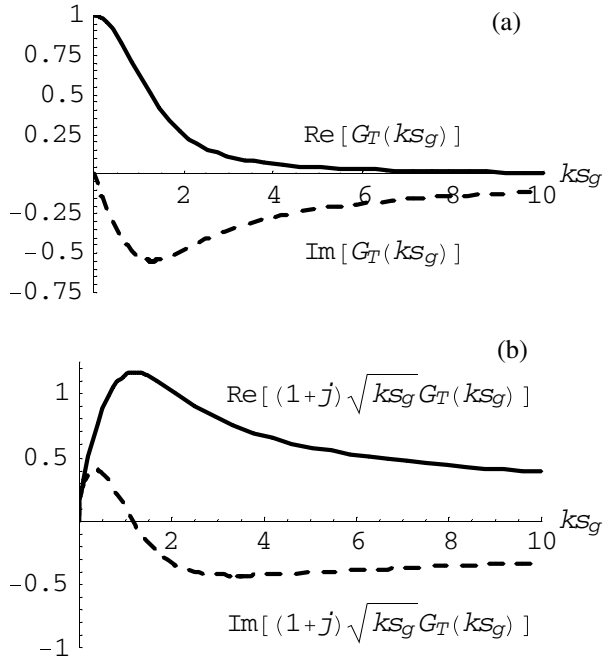

FIG. 2. (a) The real (solid curve) and imaginary (dashed curve) parts of the function G_T from Eq. (1.5). (b) The real (solid curve) and imaginary (dashed curve) parts of $(1+j)\times\sqrt{ks_g}G_T(ks_g)$, which gives the frequency dependence of $Z(a,g;k)$ when $ka^2 \gg g$.

$$s_0 = \left(\frac{2a^2}{Z_0\sigma}\right)^{1/3}. \tag{1.4}$$

On the other hand, we have found that for $ka^2 \gg g$, the contribution to the impedance of the transition radiation emitted due to the discontinuity in conductivity must be included, and

$$G \cong G_T(ks_g) = (ks_g)^{-2}\left[1 - e^{-(ks_g)^2} - \frac{2jks_g}{\sqrt{\pi}} + je^{-(ks_g)^2}erfi(ks_g)\right]. \tag{1.5}$$

The imaginary error function is defined by

$$erfi(z) = -jerf(jz) = \frac{2}{\sqrt{\pi}}\int_0^z dx\exp(x^2), \tag{1.6}$$

and we have introduced the new characteristic length scale s_g by

$$s_g = \sqrt{\frac{g}{2Z_0\sigma}}. \tag{1.7}$$

The real and imaginary parts of the function G_T are plotted in Fig. 2(a) and the real and imaginary parts of $(1+j)\sqrt{ks_g}G_T(ks_g)$, which gives the frequency dependence of the impedance when $ka^2 \gg g$, in Fig. 2(b).

We have solved numerically the truncated linear algebraic equations derived in Sec. II. In Fig. 3 we plot the actual function G (solid curve) as determined numerically and the function G_T (dashed curve) as given in Eq. (1.5). As expected, G_T is a good approximation in the transient regime $ka^2 \gg g$ but not in the equilibrium regime $ka^2 \ll g$. In Fig. 4 we plot the actual function G (solid curve) and the function G_∞ as given in Eq. (1.3). We see that, as expected, G_∞ is a good approximation in the equilibrium regime $ka^2 \ll g$ but not in the transient regime $ka^2 \gg g$. (Note that although the real part of the impedance must be positive, the ReG can have either sign.)

As an example to illustrate the order of magnitude of the key parameters, let us consider a copper resistor with $\sigma = 6\times10^7\ (\Omega\,\mathrm{m})^{-1}$, $g = 1$ m, and $a = 0.01$ m. In this case, $s_g = 5\ \mu$m and $s_0 = 20\ \mu$m, so the impedance of Eq. (1.5) holds for $ks_g \gg 0.05$. If the material is stainless steel with $\sigma = 1.4\times10^6\ (\Omega\,\mathrm{m})^{-1}$, then $s_g = 31\ \mu$m and $s_0 = 72\ \mu$m and Eq. (1.5) holds for $ks_g \gg 0.31$.

This paper is organized as follows: In Sec. II we derive the integral equation determining the longitudinal electric field in the resistor. Expanding the field in a Fourier series in the axial coordinate z, the integral equation is rewritten as an infinite set of linear algebraic equations for the Fourier coefficients. Truncating these equations by keeping only a limited number of Fourier coefficients, the equations are solved numerically. In Sec. III we consider the impedance in the high frequency limit, $ka \gg 1$, and derive a simpler integral equation for the electric field in the resistor which holds when $ka^2 \gg g$. We solve this equation analytically, thus obtaining the impedance in the transient regime. From this approximation to the impedance, we compute the short-range wakefield

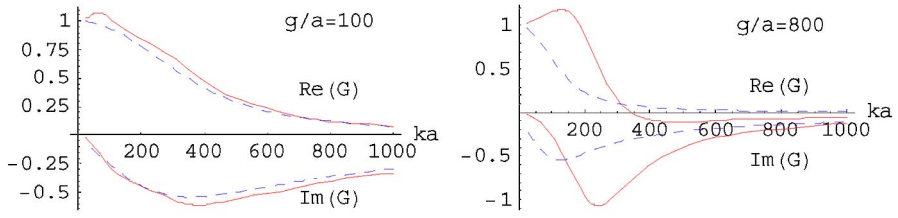

FIG. 3. (Color) The dashed curves representing the transient approximation G_T [Eq. (1.5)] are seen to be in agreement with the solid curves representing the real and imaginary parts of the function G as determined from a numerical solution of the truncated linear algebraic equations when $ka \gg g/a$. Results are for $a = 0.01$ m and $\sigma = 10^6\ (\mathrm{ohm\,m})^{-1}$.

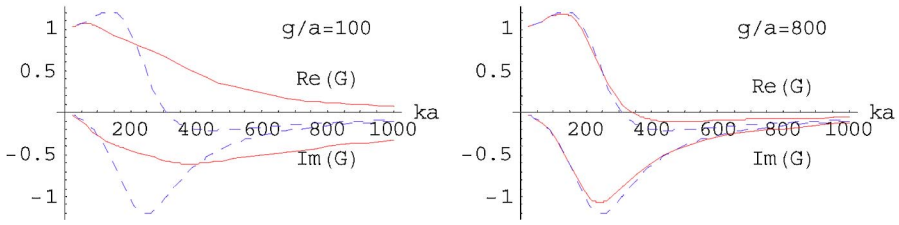

FIG. 4. (Color) The dashed curves representing the equilibrium approximation G_∞ [Eq. (1.3)] are seen to be in agreement with the solid curves representing the real and imaginary parts of the function G as determined from a numerical solution of the truncated linear algebraic equations when $ka \ll g/a$. Results are for $a = 0.01$ m and $\sigma = 10^6$ (ohm m)$^{-1}$.

(Sec. IV), the energy loss factor (Sec. V), and the transverse kick factor (Sec. VI). We conclude in Sec. VII with some final remarks.

II. DERIVATION OF INTEGRAL EQUATION

Consider a cylindrical tube (Fig. 1) of radius a, with finite conductivity σ $(0 < z < g)$ and infinite conductivity outside this interval. We shall calculate the longitudinal impedance $Z(k)$ by applying the approach developed in Ref. [7]. Assuming all time dependence is given by $\exp(j\omega t)$, the fields in the tube can be expressed as

$$H_\phi = \frac{I_0 e^{-jkz}}{2\pi r} + \frac{jk}{Z_0}\int dq e^{-jqz}\frac{J_1(Kr)}{KJ_0(Ka)}A(q), \tag{2.1}$$

$$E_z = \int dq e^{-jqz}\frac{J_0(Kr)}{J_0(Ka)}A(q), \tag{2.2}$$

where $K = \sqrt{k^2 - q^2}$. The impedance is determined by

$$Z(k) = \frac{-1}{I_0}\int_0^g dz E_z(r = a, z)e^{jkz}. \tag{2.3}$$

When the skin depth is small compared to the tube radius $(ka^2 \gg 1/\sigma Z_0)$, and assuming thick enough pipe compared to the skin depth, the boundary condition can be well approximated by

$$E_z(r = a, z) = \begin{cases} -Z_s(k)H_\phi(r = a, z) & (0 < z < g) \\ 0 & \text{otherwise,} \end{cases} \tag{2.4}$$

where

$$Z_s(k) = (1 + j)Z_0\sqrt{\frac{k}{2\sigma Z_0}}. \tag{2.5}$$

Using Eqs. (2.1) and (2.2) in the boundary condition of Eq. (2.4), we find the integral equation

$$f(z) = -\frac{Z_s I_0 e^{-jkz}}{2\pi a} + \frac{Z_s jka}{2\pi Z_0}\int_0^g dz' K_p(z - z')f(z'), \tag{2.6}$$

where $f(z) = E_z(r = a, z)$ and the pipe kernel is

$$K_p(z - z') \equiv -\int dq \frac{J_1(Ka)}{KaJ_0(Ka)}e^{jq(z-z')} = \frac{2\pi j}{a}\sum_{s=1}^{\infty}\frac{e^{-jb_s|z-z'|/a}}{b_s}, \tag{2.7}$$

with $b_s^2 = k^2a^2 - \mu_s^2$ and $J_0(\mu_s) = 0$.

We define

$$f(z) = -\frac{Z_s I_0 e^{-jkz}}{2\pi a}F(z) \tag{2.8}$$

and

$$\hat{K}(z - z') = \sum_{s=1}^{\infty}\frac{e^{-jb_s|z-z'|/a}}{b_s}e^{jk(z-z')}. \tag{2.9}$$

In Eq. (2.9), the normalization of the kernel is slightly different than that used in Ref. [7]. The integral equation can be written in the form

$$F(z) = 1 - \frac{Z_s(k)k}{Z_0}\int_0^g dz'\hat{K}(z - z')F(z'), \tag{2.10}$$

and the impedance is determined by

$$Z(k) = \frac{Z_s(k)}{2\pi a}\int_0^g dz F(z). \tag{2.11}$$

Let us now define the dimensionless variables

$$p = ka, \qquad d = g/a, \qquad x = z/a, \tag{2.12}$$

and

$$\lambda = \frac{Z_s(k)ka}{Z_0} = \frac{(1 + j)(ks_0)^{3/2}}{2}. \tag{2.13}$$

The integral equation can now be written as

$$F(x) = 1 - \lambda\int_0^d dx\hat{K}(x - x')F(x'). \tag{2.14}$$

Introducing the Fourier expansion

$$F(x) = \sum_{m=-\infty}^{\infty} C_m e^{j2\pi mx/d}, \tag{2.15}$$

the integral equation (2.14) reduces to an infinite set of linear equations for the Fourier coefficients C_n,

$$\sum_{n=-\infty}^{\infty} (\delta_{mn} + \lambda d K_{mn}) C_n = \delta_{m0}. \tag{2.16}$$

The matrix elements,

$$K_{mn} = \frac{1}{d^2}\int_0^d dx \int_0^d dx' \hat{K}(x-x') e^{-j2\pi m x/d} e^{j2\pi n x'/d} = K^{(1)}_{mn} + K^{(2)}_{mn}, \tag{2.17}$$

are given by

$$K^{(1)}_{mn} = \sum_{s=1}^{\infty} \frac{1}{b_s}\left[\frac{1 - e^{-j(db_s - dp)}}{(db_s - dp + 2\pi m)(db_s - dp + 2\pi n)} + \frac{1 - e^{-j(db_s + dp)}}{(db_s + dp - 2\pi m)(db_s + dp - 2\pi n)}\right], \tag{2.18}$$

$$K^{(2)}_{mn} = \sum_{s=1}^{\infty} \frac{-j\delta_{mn}}{b_s}\left[\frac{1}{db_s - dp + 2\pi n} + \frac{1}{db_s + dp - 2\pi n}\right]. \tag{2.19}$$

The sum in Eq. (2.19) can be performed yielding

$$K^{(2)}_{mn} = \frac{jJ_1(\sqrt{\xi_n})\delta_{mn}}{d\sqrt{\xi_n} J_0(\sqrt{\xi_n})}, \qquad (\xi_n > 0), \tag{2.20a}$$

$$K^{(2)}_{mn} = \frac{jI_1(\sqrt{-\xi_n})\delta_{mn}}{d\sqrt{-\xi_n} I_0(\sqrt{-\xi_n})}, \qquad (\xi_n < 0), \tag{2.20b}$$

$$K^{(2)}_{mn} = \frac{j\delta_{mn}}{2d}, \qquad (\xi_n = 0), \tag{2.20c}$$

where $\xi_n = \frac{4\pi n}{d}(p - \frac{\pi n}{d})$. The impedance is determined by the zero Fourier component C_0. Writing the impedance in the form of Eq. (1.1), we see that

$$G = C_0. \tag{2.21}$$

Keeping only a finite number of Fourier coefficients C_n and truncating the sum over the zeros of the Bessel function, we have solved the linear equations (2.16) for C_0 and hence determined the impedance. A similar approach has recently been applied to a related problem in Ref. [8].

III. BEHAVIOR OF IMPEDANCE FOR $ka^2 \gg g$

For $p = ka \gg 1$, consider the matrix elements $K^{(1)}_{mn}$ and $K^{(2)}_{mn}$ in Eqs. (2.18) and (2.19). Recall that $b_s = \sqrt{p^2 - \mu_s^2}$. For large p, we can approximate

$$b_s - p \cong \frac{-\mu_s^2}{2p}. \tag{3.1}$$

We see that the first term in the sums will dominate and for $p \gg 1$,

$$K^{(1)}_{mn} \cong \sum_{s=1}^{\infty} \frac{1}{p}\left[\frac{1 - \exp(jd\mu_s^2/2p)}{(\frac{d\mu_s^2}{2p} - 2\pi m)(\frac{d\mu_s^2}{2p} - 2\pi n)}\right] \tag{3.2}$$

and

$$K^{(2)}_{mn} \cong \sum_{s=1}^{\infty} \frac{j\delta_{mn}}{b_s} \frac{1}{\frac{d\mu_s^2}{2p} - 2\pi n}. \tag{3.3}$$

Carrying out an inverse Fourier transform, we can return to the integral equation (2.14). Using Eq. (2.17), it is straightforward to check that the approximate matrix elements given in Eqs. (3.2) and (3.3) correspond to the approximate kernel, $\hat{K}_a(x)$, where

$$\hat{K}_a(x) = \begin{cases} \frac{1}{p}\sum_{s=1}^{\infty} \exp(\frac{jx\mu_s^2}{2p}) & (x > 0) \\ 0 & (x < 0). \end{cases} \tag{3.4}$$

Gluckstern [7] has previously discussed this approximation to the pipe kernel valid for $p \gg 1$. He found that for $p \gg d$, the sum over s can be approximated by an integral to obtain

$$\hat{K}_a(x) \cong \begin{cases} \frac{1+j}{2\pi}\sqrt{\frac{\pi}{px}} & (x > 0) \\ 0 & (x < 0). \end{cases} \tag{3.5}$$

In this case, $(ka \gg g/a)$, the integral equation (2.14) can be approximated by

$$F(x) = 1 - \Lambda \int_0^x dx' \frac{F(x')}{\sqrt{x - x'}} \qquad (0 \le x \le d), \tag{3.6}$$

where

$$\Lambda = \frac{(1+j)Z_s(k)\sqrt{ka}}{2\sqrt{\pi} Z_0}. \tag{3.7}$$

Iterating the kernel, we find the solution

$$F(x) = \exp(-\kappa x) - \frac{j}{\sqrt{\pi}}\sqrt{\kappa x}\, h(\kappa x), \tag{3.8}$$

with

$$\kappa = -\pi\Lambda^2 = \frac{k^2 a}{2Z_0\sigma} \tag{3.9}$$

and

$$h(y) = \int_0^1 du \frac{\exp(-uy)}{\sqrt{1-u}} = \sum_{m=0}^{\infty} \frac{(-)^m 2^{m+1} y^m}{(2m+1)!!}. \tag{3.10}$$

We can also express the function h in terms of the imaginary error function,

$$h(y) = \sqrt{\frac{\pi}{y}} e^{-y} erfi(\sqrt{y}). \tag{3.10a}$$

We see that $h(y) \approx 1/y$ $(y \gg 1)$. The impedance [Eq. (2.11)] is given by $(ka \gg g/a)$

$$Z(k) \cong \frac{Z_s(k)}{2\pi} \int_0^d dx \left[\exp(-\kappa x) - j\sqrt{\frac{\kappa x}{\pi}} h(\kappa x) \right]. \quad (3.11)$$

Let us write $\kappa d = (k s_g)^2$, where

$$s_g = \left(\frac{g}{2Z_0\sigma}\right)^{1/2}. \quad (3.12)$$

Performing one of the integrations in Eq. (3.11), we find

$$Z(k) \cong \frac{Z_s(k) g}{2\pi a} G_T(k s_g), \quad (3.13)$$

where

$$G_T(u) = \int_0^1 dx e^{-u^2 x} \left[1 - \frac{2ju}{\sqrt{\pi}} \sqrt{1-x} \right] = u^{-2} \left[1 - e^{-u^2} - \frac{2ju}{\sqrt{\pi}} + j e^{-u^2} erfi(u) \right] \quad (3.14)$$

is plotted in Fig. 2. This approximation to the impedance only holds for high frequencies satisfying

$$k a^2 \gg g. \quad (3.15a)$$

Noting that $\frac{ka^2}{g} = \frac{(ks_0)^3}{(2ks_g)^2}$, this inequality can be rewritten in two equivalent but illuminating forms:

$$k s_g \gg 4(s_g/s_0)^3 \quad (3.15b)$$

and

$$k s_g \ll \frac{1}{2}(k s_0)^{3/2}. \quad (3.15c)$$

The inequality (3.15b) shows that when $s_g < s_0$ the approximate impedance of Eq. (3.13) applies over a broad frequency range. On the other hand, when $s_g > s_0$, Eq. (3.13) only holds for frequencies large compared to $1/s_g$. As we shall discuss a little later, the inequality (3.15c) is the condition for the asymptotic behavior given by Eq. (3.13) to dominate over that determined by Bane and Sands [3] for an infinite tube with finite conductivity.

One can easily show that

$$G_T(u) \approx 1 - \frac{4ju}{3\sqrt{\pi}} \qquad (u \ll 1) \quad (3.16)$$

and

$$G_T(u) \approx \frac{1}{u^2} - \frac{2j}{\sqrt{\pi}} \left(\frac{1}{u} - \frac{1}{2u^3} - \frac{1}{4u^5} - \cdots \right) \qquad (u \gg 1). \quad (3.17)$$

A rough approximation for $G_T(u)$ satisfying the leading behavior for small and large argument is the resonant form

$$G_T(k s_g) \cong \frac{1}{1 + j k s_g (\sqrt{\pi}/2)}. \quad (3.18)$$

When $k s_g \ll 1$, which requires $s_g < s_0$ as is clear from the inequality (3.15b),

$$Z(k) \cong \frac{Z_s(k) g}{2\pi a} \left[1 - \frac{j}{\sqrt{\pi}} \frac{4}{3} (k s_g) \right]. \quad (3.19)$$

The first term is the usual low frequency form of the resistive wall impedance.

When $k \gg \max[1/s_g, g/a^2]$,

$$Z(k) \cong \frac{2Z_0(1-j)}{2\pi a} \sqrt{\frac{g}{\pi k}} + \frac{Z_0(1+j)}{\pi} (k s_0)^{-3/2}. \quad (3.20)$$

Note that the leading term for high frequency is proportional to the square root of the resistor length and independent of the conductivity. Of course, the frequency range over which this asymptotic form holds depends on the conductivity. The leading term is twice that given by the diffraction impedance model ([1,2], and references therein) for a cavity of length g in a beam pipe of radius a.

For a cylindrical tube having finite conductivity and infinite length, the impedance is that discussed by Bane and Sands [3] and

$$G \cong G_\infty(k s_0) = \frac{1}{1 + \frac{1}{4}(j-1)(k s_0)^{3/2}}. \quad (3.21)$$

Comparing the approximation of $G_T(k s_g)$ given in Eq. (3.18) with $G_\infty(k s_0)$ of Eq. (3.21) suggests that the Bane and Sands approximation will be valid for $k s_g \gg \frac{1}{2}(k s_0)^{3/2}$ (i.e., $g \gg k a^2$) and our new result [Eq. (3.13)] for the high frequency impedance of a finite-length resistor will hold for $k s_g \ll \frac{1}{2}(k s_0)^{3/2}$ (i.e., $g \ll k a^2$).

IV. WAKEFIELD

The impedance is the Fourier transform of the wakefield $w(s)$. It follows from causality that the wake vanishes in front of the driving particle. Therefore, we can write

$$Z(k) = \int_0^\infty \frac{ds}{c} e^{-jks} w(s) = \int_0^\infty \frac{ds}{c} \cos(ks) w(s) - j \int_0^\infty \frac{ds}{c} \sin(ks) w(s). \quad (4.1)$$

Using the inverse cosine or sine transform, we can express the wakefield in terms of either the real or imaginary part of the impedance via

$$w(s) = \frac{2c}{\pi} \int_0^\infty dk \cos(ks) \mathrm{Re} Z(k) = -\frac{2c}{\pi} \int_0^\infty dk \sin(ks) \mathrm{Im} Z(k). \quad (4.2)$$

When $s_g < s_0$, the impedance of Eq. (3.13) is a good approximation over the wide range of frequencies given by the inequality (3.15b), including values with $k \ll 1/s_g$ as well as $k \gg 1/s_g$. In this case, the wakefield is well

approximated by inserting the impedance of Eq. (3.13) into Eq. (4.2). In this manner we obtain

$$w(s) = \frac{cg}{\pi^2 a}\frac{Z_0}{\sqrt{2s_g^3 Z_0 \sigma}} W_T\left(\frac{s}{s_g}\right), \tag{4.3}$$

where

$$W_T(\alpha) = \int_0^\infty du \cos(u\alpha) u^{-3/2}\left[1 - e^{-u^2} + \frac{2u}{\sqrt{\pi}} - e^{-u^2} erfi(u)\right] \tag{4.4a}$$

$$= -\int_0^\infty du \sin(u\alpha) u^{-3/2}\left[1 - e^{-u^2} - \frac{2u}{\sqrt{\pi}} + e^{-u^2} erfi(u)\right]. \tag{4.4b}$$

We have verified that the two integrals in Eqs. (4.4a) and (4.4b) are equal, which demonstrates that the wakefield derived from the approximate impedance of Eqs. (3.13) vanishes in front of the particle as required by causality. Support for equality was obtained in two ways: (i) by numerical integration and (ii) by showing that the two expressions have the same asymptotic expansion for large α.

The function W_T is plotted in Fig. 5. The behavior for small argument is given by

$$W_T(\alpha) = \sqrt{\frac{2}{\alpha}} - \sqrt{2\pi\alpha} + \frac{2\sqrt{2}}{3}\alpha^{3/2} + O(\alpha^{5/2}). \tag{4.5}$$

The large argument behavior is described by the asymptotically convergent series

$$W_T(\alpha) \approx \frac{-1}{\sqrt{2}} \sum_{n=0}^{\infty} \frac{\Gamma(n+3/2)}{\alpha^{n+3/2}\Gamma(\frac{n}{2}+2)}. \tag{4.6}$$

One can show from Eq. (4.4a) that $\int_0^\infty d\alpha W_T(\alpha) = 0$, implying that the area under the curve in Fig. 5 vanishes.

When $s_g > s_0$, the impedance of Eq. (3.13) is a good approximation only for $k \gg 1/s_g$. In this case, one must use a more accurate description of the impedance to determine the long range part of the wake.

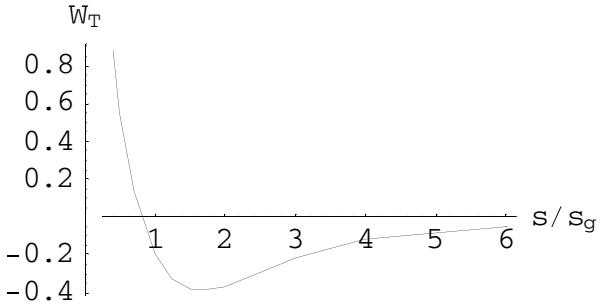

FIG. 5. The function W_T appearing in Eq. (4.3).

V. ENERGY LOSS FACTOR

We consider a Gaussian bunch with total charge Q and rms bunch length σ_s. We assume that $s_g < s_0$ and $\sigma_s \ll a^2/g$ are satisfied. The longitudinal loss factor is defined to be the energy loss of the bunch divided by the square of the bunch charge,

$$\kappa_l = -\Delta W/Q^2 = \frac{c}{\pi}\int_0^\infty dk \mathrm{Re}Z(k) e^{-k^2\sigma_s^2}. \tag{5.1}$$

Using the impedance of Eqs. (3.13) and (3.14) in (5.1), we find

$$\kappa_l = \frac{cZ_0 g\Gamma(3/4)}{4\pi^2 a\sqrt{2\sigma Z_0}s_g^{3/2}} K_l\left(\frac{\sigma_s}{s_g}\right), \tag{5.2}$$

where [see Fig. 6]

$$K_l(u) = \frac{2}{\Gamma(3/4)}\int_0^\infty dx x^{-3/2} e^{-x^2u^2}\left[1 - e^{-x^2} + \frac{2x}{\sqrt{\pi}} - e^{-x^2} erfi(x)\right]. \tag{5.3}$$

In the long bunch limit,

$$K_l(u) \approx u^{-3/2} \qquad (u \to \infty), \tag{5.4}$$

and the loss factor per unit length goes to the well-known expression for the infinite-length resistor [2]

$$\kappa_l/g = \kappa_l^\infty = \frac{cZ_0\Gamma(3/4)}{4\pi^2 a\sqrt{2\sigma Z_0}\sigma_s^{3/2}}, \qquad \sigma_s \gg s_g. \tag{5.5}$$

The short bunch case is more interesting. Here,

$$K_l(u) \approx \frac{2\Gamma(1/4)}{\sqrt{\pi}\Gamma(3/4)}\frac{1}{\sqrt{u}} \cong \frac{3.34}{\sqrt{u}} \qquad (u \to 0) \tag{5.6}$$

and the loss factor is given by

$$\kappa_l = \frac{cZ_0\sqrt{g}\Gamma(1/4)}{2\pi^{5/2}a\sqrt{\sigma_s}}, \qquad \sigma_s \ll s_g. \tag{5.7}$$

Hence, in this regime the loss factor is proportional to the

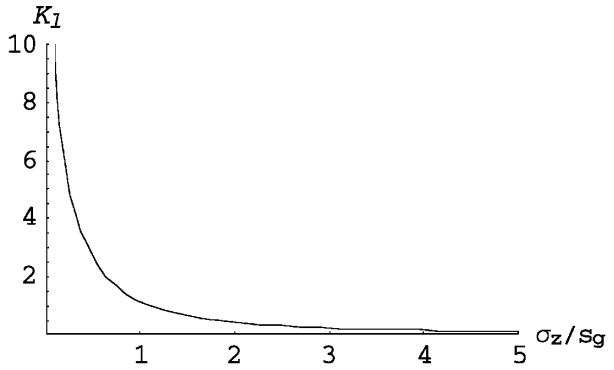

FIG. 6. The function $K_l(\sigma_s/s_g)$ which determines the loss factor.

square root of the resistor length g and is independent of conductivity which is also the case for the diffraction model.

VI. TRANSVERSE KICK FACTOR

Following the analysis of Ref. [9], we have verified that for $ka \gg 1$ and $ka^2 \gg g$ the transverse ($m = 1$) impedance $Z_t(k)$ is related to the longitudinal ($m = 0$) impedance $Z(k)$ by the well-known relation

$$Z_t(k) = \frac{2}{ka^2} Z(k). \tag{6.1}$$

The kick factor κ_t is defined by relating the angular deflection of the centroid of the bunch to its displacement via

$$\Delta y' = \frac{4\pi N\, r_e}{Z_0 c\gamma} \kappa_t y, \tag{6.2}$$

where $r_e = \frac{e^2}{4\pi\varepsilon_0 mc^2}$ is the classical electron radius, and N is the number of particles in a bunch. The kick factor is expressed in terms of the transverse impedance by [10]

$$\kappa_t = c \int_0^\infty dk\, \Phi(k\sigma_s) \mathrm{Re} Z_t(k), \tag{6.3}$$

where

$$\Phi(x) = \frac{1}{\pi} e^{-x^2} erfi(x). \tag{6.4}$$

Finding the real part of the transverse impedance by inserting the real part of the longitudinal impedance specified in Eqs. (3.13) and (3.14) into Eq. (6.1), and using the result in (6.3), we find

$$\kappa_t = \frac{cZ_0\sqrt{gs_g}\Gamma(1/4)}{2\pi^2 a^3} K_t\left(\frac{\sigma_s}{s_g}\right), \tag{6.5}$$

with

$$K_t(u) = \frac{2}{\Gamma(1/4)} \int_0^\infty dx\, x^{-5/2} e^{-u^2x^2} erfi(ux)\Big[1 - e^{-x^2} + \frac{2x}{\sqrt{\pi}} - e^{-x^2} erfi(x)\Big]. \tag{6.6}$$

The function $K_t(u)$is plotted in Fig. 7.

The limiting behavior of the kick factor for long bunch length is given by

$$K_t(u) \approx u^{-1/2} \qquad (u \to \infty), \tag{6.7}$$

and for short bunch length by

$$K_t(u) \approx \frac{8\Gamma(3/4)\sqrt{u}}{\sqrt{\pi}\Gamma(1/4)} \cong 1.52\sqrt{u} \qquad (u \to 0). \tag{6.8}$$

Hence, in the long bunch limit, the kick factor is given by the well-known expression for the kick factor per unit length for an infinite resistor [2,11]

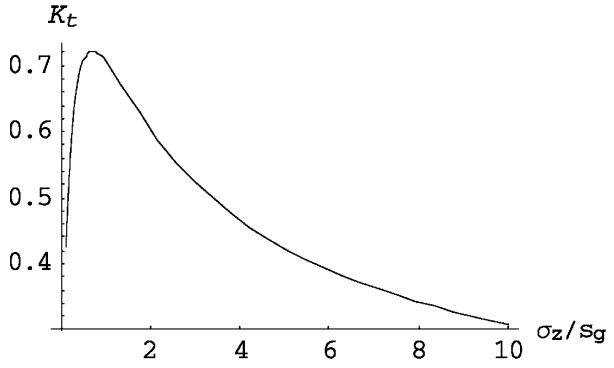

FIG. 7. The function $K_t(\sigma_s/s_g)$ which determines the transverse kick factor.

$$\kappa_t/g = \kappa_t^\infty = \frac{cZ_0\Gamma(1/4)}{(2\pi)^{3/2}a^3\sqrt{\pi\sigma Z_0\sigma_s}}, \qquad \sigma_s \gg s_g, \tag{6.9}$$

while in the short bunch limit the kick factor is given by

$$\kappa_t = \frac{4\Gamma(3/4)}{\pi^{5/2}} \frac{cZ_0\sqrt{g\sigma_s}}{a^3}, \qquad \sigma_s \ll s_g. \tag{6.10}$$

VII. CONCLUDING REMARKS

We have considered the impedance of a finite length resistive pipe in axially symmetric geometry. The main results of our paper can be summarized as follows. When the Rayleigh range of a mode with wave number k and radius a is large compared to the length of the resistor ($ka^2 \gg g$), the behavior of the impedance can differ significantly from that of a resistor of infinite length. A new length scale s_g [Eq. (1.7)] enters the problem. For $k \ll 1/s_g$, the longitudinal impedance is given by the low frequency resistive wall impedance,

$$Z(k) \cong \frac{Z_s(k)g}{2\pi a}. \tag{7.1}$$

For $k \gg 1/s_g$, the high frequency asymptotic behavior [Eq. (3.20)] is twice that given by the diffraction impedance model ([1,2], and references therein) for a cavity of length g in a beam pipe of radius a,

$$Z(k) \cong (1 - j)\frac{2Z_0}{2\pi a}\sqrt{\frac{g}{\pi k}}. \tag{7.2}$$

The low frequency resistive wall impedance cannot continue to very high frequencies because the corresponding negative wakefield would result in acceleration of the particles trailing immediately behind the leading particle [2]. The diffraction model, on the other hand, yields a proper retarding wakefield immediately behind the leading particle. Therefore, it is reasonable that at some sufficiently high frequency the diffraction-model-like behavior becomes dominant. The value of k for which

the magnitudes of the two asymptotic forms given in (7.1) and (7.2) becomes equal is (up to a constant of the order of 1) the inverse of the characteristic length scale s_g.

Since this paper primarily deals with the behavior of the high frequency impedance, a few remarks on the high frequency limitations of our treatment are in order. First of all, as is true for any impedance, the finite length resistive wall impedance considered here will fall off exponentially at wave numbers that exceed $k_{c\gamma} \sim \gamma/a$. Also, the normal skin effect expression for the surface impedance Eq. (1.2) breaks down at high frequencies due to either anomalous skin effect [12] or relaxation effects [3]. This typically occurs at very high frequencies and is ignored in this paper.

While our theory is formally applicable when $s_g < s_0$, significant corrections to the usual long-bunch infinite-length resistor consideration only appear at frequencies $k \sim s_g^{-1}$ and higher. In order for these frequencies to significantly overlap with the single bunch spectrum, one has to have $k \sim 1/\sigma_s$, where σ_s is rms bunch length. Since s_g is typically very small, our theory is relevant for very short bunches $\sigma_s \leq s_g$.

We have considered an idealized geometry as well as assuming outer pipes of infinite conductivity. In a typical accelerator environment, a step change in conductivity associated with devices such as collimators, minigap undulators, etc., is often accompanied by a cross-section change. While the changes in conductivity and cross section act on a beam together, our idealized treatment gives some insight and permits order of magnitude estimates for the effect of the resistive part alone when the element is short enough, $g \ll a^2/\sigma_s$.

On the other hand, high resistance elements without a change in the vacuum chamber cross section do sometimes occur in accelerators. One example is a short stainless steel insert in a low resistivity vacuum chamber, which is used for high speed magnet correctors [low conductivity allows fast (~ 100 Hz) magnetic fields to penetrate the chamber]. We believe that our treatment very closely applies to this situation, and in fact, if bunches are short enough, the effect on the beam could be very different from what results from existing theories. Another commonly used element is a short piece of ceramic typically used to accommodate fast kickers. While the surface impedance of ceramic is different from what has been considered in this paper, we believe this problem is tractable with a similar formalism.

Consider a 25 cm long stainless steel insert in a 1 cm radius low resistivity chamber. From the example given in the Introduction, $s_g \sim 15$ μm and $s_0 \sim 72$ μm so our theory applies well. For 8 μm rms long bunch, i.e., $\sigma_s \sim 0.5 s_g$, Eqs. (6.5) and (6.6) give the kick factor of about 29 V/(pC m). Let us compare this kick factor to the predictions one would get based on the infinite-length resistor impedance of Eqs. (1.1) and (1.3). Of course, since $a^2 \gg g\sigma_s$ the infinite-length impedance should not be applied to this particular case. In a manner similar to the derivation of Eq. (6.5) and (6.6), we can calculate the kick factor directly from the infinite-length impedance. This results in a kick factor of 7.5 V/(pC m), i.e., an underestimate of almost a factor of 4. Hence, for short bunches the effect of finite length can be pronounced.

Finally, we note that while an accurate measurement of the effect of the resistive wake of a finite element on a beam is a nontrivial matter, it was recently successfully measured at SLAC using the SLC beam at 1.2 GeV [13]. A transverse kick to the beam after passing through a tapered graphite collimator was measured and the geometric effects were accounted for by repeating the measurements on an identical copper collimator. Because of a relatively long bunch ($\sigma_s = 650$ μm $\gg s_g, s_0$) our theory does not directly apply (or predict anything of importance) to this case (even when ignoring the flat geometry and the effect of tapers). For this case the kick factor can be calculated from the analog of Eq. (6.9) for a parallel-plate geometry, as it was in fact done in [13].

However, we predict that if this experiment is repeated with a much shorter bunch, for example $\sigma_s = 20$ μm which is equal to the LCLS bunch length [14], the finite length aspect of the resistive wall impedance will be very pronounced. In fact, for such a short bunch, one does not need to go to graphite, and the transverse kick from a 25 cm long stainless steel insert in a 1 cm radius round chamber should be measurable. To convincingly observe the characteristic behavior in the finite-length regime, one could, for example, measure the kick to the bunch at several insert lengths. Lengthening the insert by a factor of 4 (from 25 cm to 1 m) should result in a total kick increase of only a factor of 3, which should be easily distinguished from the linear dependence predicted by the theory for an infinite-length resistor.

ACKNOWLEDGMENTS

We thank K. Bane, G. Stupakov, and B. Zotter for stimulating discussions on the behavior of impedance at high frequency. This work was supported by Department of Energy Contract No. DE-AC02-98CH10886. R. L. G. is also grateful to DOE for partial support during the course of this work.

[1] R. B. Palmer, Part. Accel. **25**, 97 (1990).
[2] A. W. Chao, *Physics of Collective Beam Instabilities in High Energy Accelerators* (Wiley, New York, 1993).
[3] K. L. F. Bane and M. Sands, in *Micro Bunches Workshop*, edited by E. B. Blum, M. Dienes, and J. B. Murphy, AIP Conf. Proc. No. 367 (AIP, New York, 1996), p. 131; see also K. L. F. Bane, SLAC Report No. SLAC-AP-87, 1991.

[4] H. Henke and O. Napoly, in *Proceedings of the European Particle Accelerator Conference, Nice, 1990* (Editions Frontíeres, Gif-sur-Yvette, France, 1990), p. 1046.
[5] O. Henry and O. Napoly, Part. Accel. **35**, 235 (1991).
[6] M. Ivanyan and Tsakanov, in *Proceedings of the European Particle Accelerator Conference, Paris, 2002* (EPS-IGA and CERN, Geneva, 2002), p. 1511.
[7] R. L. Gluckstern, Phys. Rev. D **39**, 2773 (1989).
[8] R. L. Gluckstern and B. Zotter (unpublished).
[9] A. V. Fedotov, R. L. Gluckstern, and M. Venturini, Phys. Rev. ST Accel. Beams **2**, 064401 (1999).
[10] G. Stupakov, SLAC Report No. SLAC-PUB-7167, 1996.
[11] A. Piwinski, DESY Report No. 94-068, 1994.
[12] G. E. H. Reuter and E. H. Sondheimer, Proc. R. Soc. London A **195**, 336 (1948).
[13] D. Onoprienko, M. Seidel, and P. Tenenbaum, in *Proceedings of the European Particle Accelerator Conference, Paris, 2002* (Ref. [6]), p. 227.
[14] Linac Coherent Light Source (LCLS) Design Study Report No. SLAC-R-521, UC-144, 1998.